



HHS Public Access

Author manuscript

ACS Sens. Author manuscript; available in PMC 2022 February 26.

Published in final edited form as:

ACS Sens. 2021 February 26; 6(2): 508–512. doi:10.1021/acssensors.0c02058.

Optical imaging of electrical and mechanical couplings between cells

Wen Shi^{1,2}, Yunze Yang¹, Ming Gao³, Jie Wu³, Nongjian Tao^{1,4}, Shaopeng Wang^{1,*}

¹Biodesign Center for Bioelectronics and Biosensors, Arizona State University, Tempe, Arizona 85287-5801, United States.

²Beijing National Laboratory for Molecular Sciences, Key Laboratory of Analytical Chemistry for Living Biosystems, Institute of Chemistry, Chinese Academy of Science, Beijing, China.

³Department of Neurobiology, St. Joseph's Hospital and Medical Center, Barrow Neurological Institute, Phoenix, AZ 85013, USA

⁴School of Electrical Computer and Energy Engineering, Arizona State University, Tempe, Arizona 85287- 5801, United States

Abstract

Intercellular communication plays a pivotal role in multicellular organisms. Studying the electrical and mechanical coupling among multiple cells has been a difficult task due to the lack of suitable techniques. In this study, we developed a label-free imaging method for monitoring the electrical-induced communications between connected cells. The method was based on monitoring the subtle mechanical motion of the cell under the electrical modulation of the membrane potential. We observed that connected cells responded to electrical modulation of neighboring cells with mechanical deformation of the membrane. We further investigated the mechanism of the coupling and confirmed that this mechanical response was induced by electrical signal communicated through the gap junction. Blocking the gap junction can temporally cease the mechanical signal

*Corresponding Author Shaopeng Wang – Biodesign Center for Bioelectronics and Biosensors, Arizona State University, Tempe, Arizona 85287-5801, United States; shaopeng.wang@asu.edu.

Wen Shi – Biodesign Center for Bioelectronics and Biosensors, Arizona State University, Tempe, Arizona 85287- 5801, United States; Beijing National Laboratory for Molecular Sciences, Key Laboratory of Analytical Chemistry for Living Biosystems, Institute of Chemistry, Chinese Academy of Science, Beijing, China 100190.

Yunze Yang – Biodesign Center for Bioelectronics and Biosensors, Arizona State University, Tempe, Arizona 85287-5801, United States

Ming Gao – Department of Neurobiology, St. Joseph's Hospital and Medical Center, Barrow Neurological Institute, Phoenix, AZ 85013, USA

Jie Wu – Department of Basic Medical Sciences, University of Arizona College of Medicine, Phoenix, AZ 85004, USA.

Nongjian Tao – Biodesign Center for Bioelectronics and Biosensors and School of Electrical Computer and Energy Engineering, Arizona State University, Tempe, Arizona 85287- 5801, United States

N.T. deceased in March 2020.

The authors declare no competing financial interest.

ASSOCIATED CONTENT

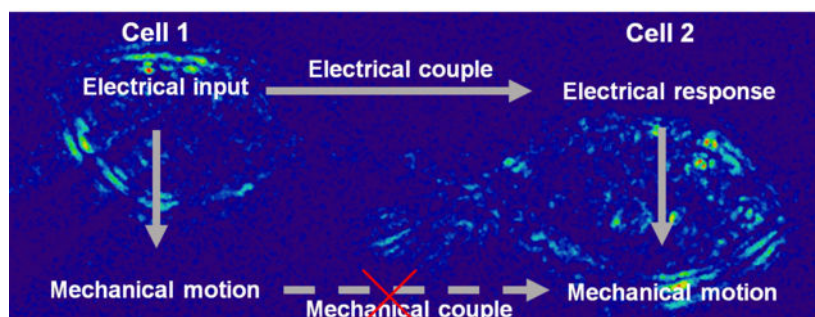
Supporting Information.

The Supporting Information is available free of charge at <https://pubs.acs.org>.

Materials and Methods: S1 cell culture; S2 procedure for imaging and modulation; S3 differential detection algorithm; S4 normalized displacement. Figure S1 scheme for differential detection algorithm; Figure S2 electrical modulated mechanical motion in A549 cells; Figure S3 mechanical motion in frequency domain; Figure S4 electrical modulated mechanical motion in multiple connected cells; Figure S5 spatial pattern of connected cell under electrical and mechanical stimulus; Figure S6 intercellular electrical couple of connected cells imaged with membrane potential sensitive dye; Figures S7 coupled motion is not observed in PC12A cells.

and this inhibition can be rescued after removing the inhibitor. This study sheds light on the mechanism of electrical coupling between neurons and provides a new method for study intercellular communications.

Graphical Abstract



Keywords

optical imaging; intercellular communication; bioelectrical signal; cell mechanical motion; HEK293T

Intercellular communication plays a pivotal role in multicellular organisms.¹ Much progress has been achieved on the basis of biomolecules, such as neurotransmitters, cytokines, DNA/RNA.^{2,3} The distribution, transmission and transform of biomolecules through cellular networks regulate cell function, induce their differentiation and finally determine their destiny.⁴ However, diverse studies have revealed the limitation of existing matter communication models, encouraging a non-specific, biophysically-oriented mechanism to add new ideas to complete the field.^{5,6} Indeed, some biophysical properties of cells have been studied intensely such as membrane potential, which has become one of the pillars of the modern neuroscience.^{7,8} Recently the bioelectrical spatial pattern is considered to be relevant to the positional information processes during embryogenesis.⁹ To date, studying the electrical coupling among multiple cells has been difficult due to the lack of suitable techniques. Although multi-patch clamp setup may be used for these studies, they are operationally challenging. Fluorescence techniques, such as membrane potential or calcium imaging, can provide important information, but the introduction of dye might lead to incognizant interference, or even toxicity to the cells.^{10,11} Therefore, there is an urgent demand for developing a label-free imaging method to study the intercellular bioelectrical communication.

In this work, we reported a label-free optical imaging method for monitoring the electrical coupling between cells. This method is based on the fact that the bioelectrical signal can trigger cellular mechanical vibration and we can detect this subtle mechanical motion with optical imaging.¹²⁻¹⁴ We have studied the coupling pattern for multiple cells through monitoring their mechanical motions under electrical stimulus. This study also revealed that the intercellular coupling is through gap junction electrically, rather than a direct mechanical coupling.

Results

To illustrate the method, two connected human embryonic kidney 293T (HEK293T) cells (defined as cell 1 and cell 2 respectively) were studied as the simplest model. We clamped the membrane potential of cell 1 at its resting voltage (-60 mV) in whole-cell configuration. Then, its membrane potential was modulated with sinusoidal electrical stimulus with an amplitude of 150 mV and frequency of 23 Hz. During these processes, the optical response of the two connected cells were recorded with bright field microscopy, from which the accompanying mechanical motions of both cells can be resolved with a differential detection algorithm (Figure 1 and supporting information section S3). As reported previously,^{15–17} this algorithm reduces the common noise of optical imaging, and can detect sub-nanometer membrane displacement, which is sensitive enough to track the mechanical motion triggered by action potential. This method is fast and allows us to monitor multiple cells simultaneously.

For example, Figure 2A shows a raw image of two connected HEK293T cells. The intensities of two crosslines on the edge of both cells were profiled at -60 mV and 90 mV respectively (Figure 2B). In both cases, the depolarization induced the troughs to move inside the cell. In addition, the difference images of each region of interest (ROI) were obtained by subtracting the images at -60 mV from those at 90 mV. A clear contrast can be observed on the edge of both cells, while the region without cell exhibited no contrast. The above results suggested a subtle lateral displacement of the membrane occurred on both cells, implying the intercellular coupling. However, due to the background noise from the physical and biological source, it is hard to portray the coupled motion on both cells by difference images directly. To solve this problem, Fast Fourier transform was used to isolate the noise from frequency domain. The FFT of the time lapse images revealed that we can only observe the intensity fluctuation at the modulation frequency (23 Hz) but not the nearby frequencies (Figure 2D), which validated that these signals were induced by the electrical modulation rather than cellular intrinsic activity from metabolism.¹² And these transformed images showed that the membrane motions were not confined to the directly stimulated cell 1 but can also be observed on cell 2, confirming the signal coupling between cells. Next, the membrane displacements were quantified through the differential algorithm. As a result, the mean displacement of cell 1 along the edge of the cell membrane was about 0.9 nm; and that of cell 2 was about 1.1 nm. In comparison, the background of the membrane motion in the absence of electrical stimulation is around 0.4 ± 0.1 nm. Similar phenomena can also be seen on other cell lines such as A549 cells (figure S2). In addition, different stimulated frequencies (23 Hz and 29 Hz) were implemented on the same cell pair and the frequency specific displacements on the cell 2 were observed (figure S3), which suggested that our method can be used to track the potential-induced intercellular coupling through membrane motions. For multiple connected cells, we detected significant membrane displacements on every cell connected (Figure S4), showing that our method is capable of label-free mapping of cellular networking activity. Moreover, we can plot the local membrane motions along the cell edge of each cell, showing significant variability of membrane displacement ranging in 0–2 nm (Figure 2D and Figure S4C), which may be attributed to the heterogeneity of the cell membrane.

From the statistics of the mean edge displacements of every cell pairs, the displacements on cell 1 is 0.5 – 1.3 nm and those on cell 2 is 0.7 – 1.4 nm. We found the membrane motions on cell 2 were probably larger than those on cell 1 (figure 3A, $p < 0.05$). However, the displacements on different cells were dispersed broadly and the background is diverse in different cell pairs, making it difficult to compare the displacements between different cell pairs. To address this issue, we used the normalized displacement (ND) to remove the background fluctuation for quantitative study of the membrane motions (Supporting Information section S4). As shown in Figure 3B, the ND distributed much narrowly for both cell 1 (from 2.1 to 4.4) and cell 2 (from 9.6 to 16.6), and the tendency that cell 2 represented more mechanical response than cell 1 was more obvious ($p < 0.001$). Moreover, positive correlation curves of the modulation voltage and the ND can be obtained in both cells, but the slope of cell 2 are sharper than that of cell 1 (figure 3C). Considering the noise of the ND in the absence of modulation, the minimum detectable modulation voltage for our method was 90 mV ($ND > 2$). The more intense displacement on the indirect modulated cell was unanticipated. This unexpected phenomenon implied the coupled motions of the cell pairs were unlikely through the direct mechanical connections, which should have shown spatial-dependent decay. Alternatively, electrical coupling might play major role for the coupled motions. The more intense motion on the indirect cell may be ascribe to the fact that the patched cell was slightly pressed by the tip of the pipette, which might confine the mobility and motion of the cell membrane. This result suggests that the mechanical effect of the patch clamp method should not be neglected when studying the electrical-mechanical coupling of biological system.

To study the mechanism of cell-to-cell signal coupling, the spatial pattern of the electrical and mechanical modulation in multiple cells was compared (figure S5). When electrical modulation was used, the mechanical responses spread among all of the connected cells, and the indirect modulated cells showed more intense motions. However, when we added only subtle mechanical vibration to the tip of the pipette, to mechanically stimulate cell 1, cell 2 (the cell connected to cell 1) showed smaller mechanical motion than cell 1, and other cells showed negligible motions. The ND distribution of mechanically stimulated cells fits to a spatial-dependent decay in damping model, confirming that the electrically stimulated membrane motions were not transmitted through direct mechanical coupling.

A reasonable explanation is that the electrical signal can transmitted between connected cells and the changing membrane potential induce mechanical motion of the local cell. To confirm this hypothesis, we measured intercellular couple of membrane potential with potential sensitive dye, di-8-ANEPPS,¹⁷ which showed that the membrane potential of the indirect modulated cell 2 responded to the change of clamped voltage of cell 1 instantaneously (Figure S6).

It has been reported that cells can be electrically coupled through gap junction.^{19,20} Meclofenamic acid (MFA) is a gap junction blocker that can be used to block neuronal type of intercellular electrical coupling.²¹ We measured the response of the connected cell pair in the presence and absent of MFA with our method. Firstly, the intact cell pair exhibited typical electrical-induced intercellular coupling; in other word, both cells were triggered by the electrical modulation while cell 2 represented mechanical response more intense than

cell 1 as envisioned (figure 4). With the addition of MFA, the coupled motion on cell 2 was remarkably inhibited, while that on cell 1 was increased dramatically. Then, after MFA was washed out, the initial coupling of the cell pair restored obviously. These results suggest that gap junction function is essential for the intercellular signal coupling.

In addition, a gap junction protein deficient cell line, PC12A cell, was investigated as a negative control,²² which showed that the cell 1 represented obvious mechanical motion, but the cell 2 displayed no responses (figure S7). These data suggested that the motion on the cell 2 came from the intercellular electrical coupling rather than the direct mechanical connection and the coupled electrical signals generated the mechanical motion locally in both cells (figure 4C).

Conclusion

In this study, we have developed an optical method for visualizing the electrical-induced communications between connected cells. The method is based on monitoring the subtle mechanical motion of the cell under the electrical modulation of the membrane potential. We find an electrical-originated and coupled mechanical response between connected cells. We further investigate the mechanism of the coupling and confirm that this intercellular communication is mediated through electrical coupling by the gap junction. Blocking gap junction with MFA will temporally cease the mechanical signal and this inhibition can be rescued after removing the inhibitor. Therefore, we confirm the gap junction mediated electrical coupling underlying the mechanism of the spreading of mechanical motions among connected cells.

Electrical and mechanical signals play key roles in cell communications. But these two components are typically coupled in neuron or cardiomyocytes communications. This is the first study to investigate the interplay between these two components. We find that the gap junction-mediated electrical connection is the key to the cell-to-cell communication. Multiple studies show that gap junction works as a node in a network to regulate the electrical signal and orchestrate the activity of the cell network. Though few is known about the regulation of mechanical coupling in cell network, these gap junctions may also play a key role in regulating mechanical signal shape and amplitude for connected cells. This study shows new clue on the mechanism of electrical coupling between neurons and provides a new method for study intercellular communications.

Supplementary Material

Refer to Web version on PubMed Central for supplementary material.

ACKNOWLEDGMENT

We acknowledge financial support from the National Institute of General Medical Sciences of the National Institutes of Health (R01GM1107165), and W.S. acknowledge financial support from National Natural Science Foundation of China (No. 21922412). We dedicate this paper to the memory of Prof. Nongjian Tao (1963–2020).

References

1. Fafián-Labora JA; O’Loughlen A Classical and nonclassical intercellular communication in senescence and ageing. *Trends Cell Biol.* 2020, 30, 628–639. [PubMed: 32505550]
2. van Niel G; D’Angelo G; Raposo G Shedding light on the cell biology of extracellular vesicles. *Nat. Rev. Mol. Cell Biol.* 2018, 19, 213–228. [PubMed: 29339798]
3. Becker A; Thakur BK; Weiss JM; Kim HS; Peinado H; Lyden D Extracellular vesicles in cancer: cell-to-cell mediators of metastasis. *Cancer Cell* 2016, 30, 836–848. [PubMed: 27960084]
4. Mathews J; Levin M Gap junctional signaling in pattern regulation: physiological network connectivity instructs growth and form. *Dev. Neurobiol.* 2016, 77, 643–673. [PubMed: 27265625]
5. Cervera J; Alcaraz A; Mafe S Bioelectrical signals and ion channels in the modeling of multicellular patterns and cancer biophysics. *Sci. Rep.* 2016, 6, 20403. DOI: 10.1038/srep20403. [PubMed: 26841954]
6. Levin M Endogenous bioelectrical networks store non-genetic patterning information during development and regeneration. *J. Physiol.* 2014, 592, 2295–2305. [PubMed: 24882814]
7. Petersen CCH Whole-cell recording of neuronal membrane potential during behavior. *Neuron* 2017, 95, 1266–1281. [PubMed: 28910617]
8. Liu P; Miller EW Electrophysiology, unplugged: imaging membrane potential with fluorescent indicators. *Acc. Chem. Res.* 2020, 53, 11–19.
9. Levin M; Pezzulo G; Finkelstein JM Endogenous bioelectric signaling networks: exploiting voltage gradients for control of growth and form. *Annu. Rev. Biomed. Eng.* 2017, 19, 353–387. [PubMed: 28633567]
10. Chemla S; Chavane F Voltage-sensitive dye imaging: technique review and models. *J. Physiol. Paris* 2010, 104, 40–50. [PubMed: 19909809]
11. Mennerick S; Chisari M; Shu HJ; Taylor A; Vasek M; Eisenman LN; Zorumski CF Diverse voltage-sensitive dyes modulate GABA_A receptor function. *J. Neurosci.* 2010, 30, 2871–2879. [PubMed: 20181584]
12. Yang YZ; Liu XW; Wang H; Yu H; Guan Y; Wang SP; Tao NJ Imaging action potential in single mammalian neurons by tracking the accompanying sub-nanometer mechanical motion. *ACS Nano.* 2018, 12, 4186–4193. [PubMed: 29570267]
13. Yang YZ; Liu XW; Wang SP; Tao NJ Plasmonic imaging of subcellular electromechanical deformation in mammalian cells. *J. Biomed. Opt.* 2019, 24, 066007. DOI: 10.1117/1.JBO.24.6.066007.
14. Zhang FN; Jing WW; Hunt A.; Yu Hui.; Yang YZ; Wang SP; Chen HY; Tao NJ. Label-free quantification of small molecule binding to membrane proteins on single cells by tracking nanometer-scale cellular membrane deformation. *ACS Nano* 2018, 12, 2056–2064. [PubMed: 29397682]
15. Guan Y; Shan XN; Zhang FN; Wang SP; Chen HY; Tao NJ Kinetics of small molecule interactions with membrane proteins in single cells measured with mechanical amplification. *Sci. Adv.* 2015, 1, e1500633. DOI: 10.1126/sciadv.1500633. [PubMed: 26601298]
16. Zhang FN; Guan Y; Yang YZ; Hunt A; Wang SP; Chen HY; Tao NJ Optical tracking of nanometer-scale cellular membrane deformation associated with single vesicle release. *ACS sensors* 2019, 4, 2205–2212. [PubMed: 31348853]
17. Yu H; Yang YT; Yang YZ; Zhang FN; Wang SP; Tao NJ Tracking fast cellular membrane dynamics with sub-nm accuracy in the normal direction. *Nanoscale* 2018, 10, 5133–5139. [PubMed: 29488990]
18. Kao WY; Davis CE; Kim YI; Beach JM Fluorescence emission spectral shift measurements of membrane potential in single cells. *Biophys. J.* 2001, 81, 1163–1170. [PubMed: 11463657]
19. Wang X; Veruki ML; Bukoreshtliev NV; Hartveit E; Gerdes HH Animal cells connected by nanotubes can be electrically coupled through interposed gap-junction channels. *Proc. Natl. Acad. Sci. U. S. A.* 2010, 107, 17194–17199. [PubMed: 20855598]
20. Ribeiro-Rodrigues TM; Martins-Marques T; Morel S; Kwak BR; Girão H Role of connexin 43 in different forms of intercellular communication—gap junctions, extracellular vesicles and tunnelling nanotubes. *J. Cell Sci.* 2017, 130, 3619–3630. [PubMed: 29025971]

21. Harks EGA; de Roos ADG; Peters PHJ; de Haan LH; Brouwer A; Ypey DL; van Zoelen EJJ; Theuvsenet APR Fenamates: a novel class of reversible gap junction blockers. *J. Pharmacol. Exp. Ther.* 2001, 298, 1033–1041. [PubMed: 11504800]
22. Bukoreshitliev NV; Wang X; Hodneland E; Gurke S; Barroso JFV; Gerdes HH Selective block of tunneling nanotube (TNT) formation inhibits intercellular organelle transfer between PC12 cells. *FEBS Lett.* 2009, 583, 1481–1488. [PubMed: 19345217]

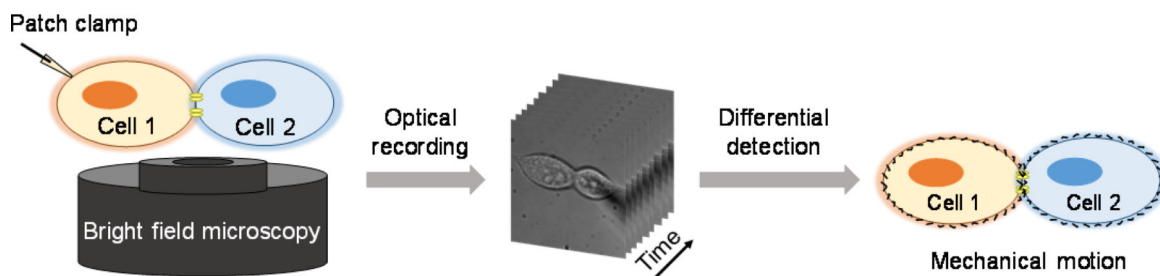


Figure 1. Schematic illustration of intercellular couple through imaging mechanical motion. The membrane potential of cell 1 is modulated in whole-cell patch clamp configuration. Bright field microscopy is used to image each cell. The electrical-induced mechanical motion of cell membrane on each cell can be resolved with a differential detection algorithm.

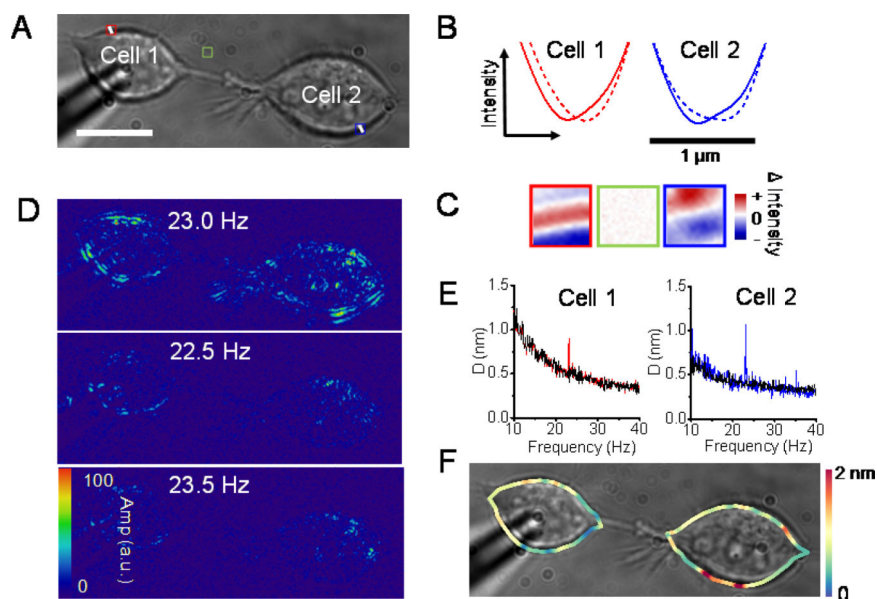


Figure 2. Electrical modulation can induce mechanical motion in both connected cells. (A) Bright field image of two connected cells. (B) The intensity of crossline on the cell edge is profiled at -60 mV (solid line) and 90 mV (dash line). The rightward arrow indicates the inside of the cells. (C) Difference images of the ROI in panel (A). (D) Difference images at 23 Hz and nearby frequencies. (E) The mean edge displacements of the cell 1 (red) and cell 2 (blue). The black curves indicate the background of the membrane motion in the absence of stimulation. (F) Edge displacement map obtained from the differential algorithm. Scale bars, 15 μm .

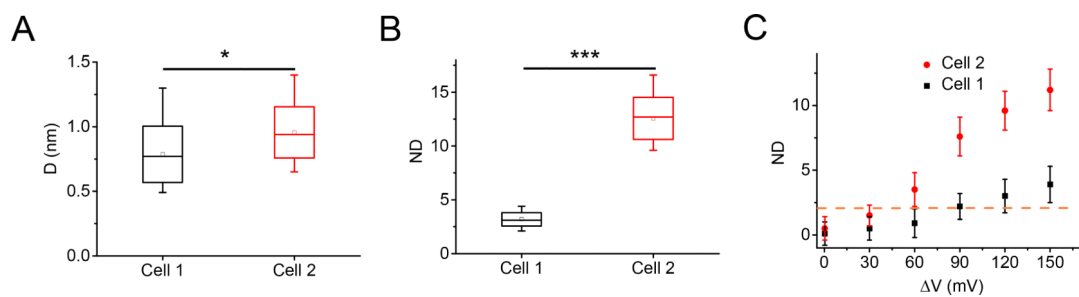


Figure 3. Quantitative analysis of the mean edge displacements in different cell pairs. (A) Statistics of the mean edge displacements of connected cell pairs. Cell pair, $n = 31$. (B) Statistics of the normalized displacements of the connected cell pairs. Cell pair, $n = 31$. (C) Normalized displacements of the connected cell pairs versus the modulation voltage. The dash line indicates $ND=2$. Cell pair, $n=4$. * $p < 0.05$, *** $p < 0.001$, two-sided Student's t -test.

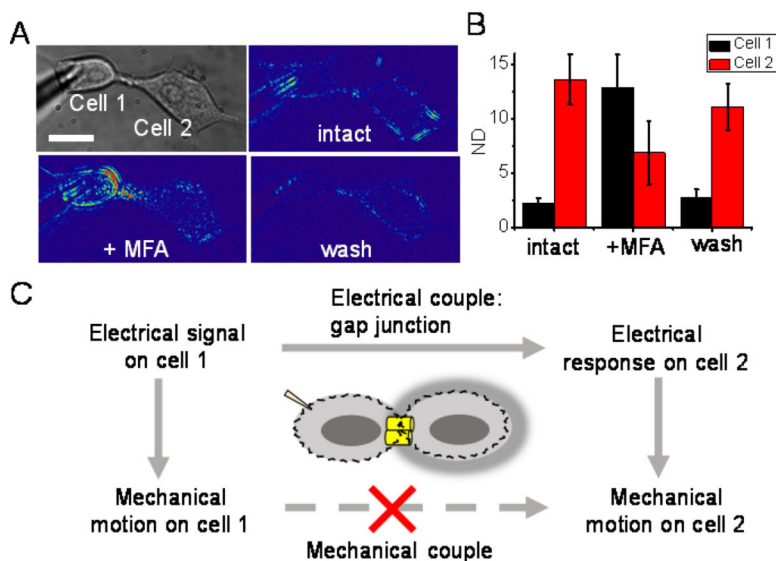


Figure 4. Gap junction participates in the intercellular couple of HEK293T cells. (A) Bright field and difference image of the cells at 23 Hz of the cells before, after addition of and after washout of MFA. Scale bar, 15 μ m. (B) The normalized displacements of cells before, after addition of and after washout of MFA. Cell pair, $n = 4$. (C) Schematic illustration of the possible pathway of intercellular couple.